# A systematic framework for the assessment of the reliability of energy supply in Integrated Energy Systems based on a quasi-steady-state model

Lixun Chi [a, b], Huai Su [a*], Enrico Zio [c, d], Meysam Qadrdan [e], Jing Zhou [a], Li Zhang [a], Lin Fan [a], Zhaoming Yang [a], Fei Xie [f], Lili Zuo [a], Jinjun Zhang [a*]

[a] National Engineering Laboratory for Pipeline Safety/ MOE Key Laboratory of Petroleum Engineering /Beijing Key Laboratory of Urban Oil and Gas Distribution Technology, China University of Petroleum-Beijing, 102249, Beijing, China

[b] PetroChina Planning & Engineering Institute, China National Petroleum Corporation, 9 Dongzhimen North Street, Dongcheng District, Beijing, P.R. China, 100007

[c] Dipartimento di Energia, Politecnico di Milano, Via La Masa 34, 20156, Milano, Italy

[d] Eminent Scholar, Department of Nuclear Engineering, College of Engineering, Kyung Hee University, Republic of Korea

[e] School of Engineering, Cardiff University, Cardiff, UK

[f] North China Branch of National Petroleum and Natural Gas Pipeline Network Group Co. LTD, 300000, Tianjin, China

[*] Corresponding author. Address: College of Mechanical and Transportation Engineering, China University of Petroleum, Fuxue Road 18, Changping District 102249, Beijing, China.
Tel.: +86-10-8973 4627; fax: +86-10-8973 4627. E-mail address: suhuai1990@163.com
Tel.: +86-10-8973 2205; fax: +86-10-8973 2205. E-mail address: zhangjj@cup.edu.cn

## Abstract

The reliability analysis of IESs (Integrated Energy Systems) is a complicated task because of the complex characteristics of different subsystems and the multi-scale dynamics that develop therein. To effectively address such problems, this paper proposes a systematic framework to analyse the reliability of energy supply in IESs, considering the dynamics of IESs and the inter-relationships among uncertainties. First, based on the linepack-based performance analysis model of IES, a quasi-steady-state model is established to model the dynamic behaviours in IESs, properly accounting for practical engineering and operational strategies. Then, considering the inter-correlations among different uncertainty sources and time-dependent relationships of each variable, a model that combines the statistical structure of copula with the machine learning method of stacked autoencoder (CSML) is adopted to establish the timely multivariate joint distributions for variables. Monte Carlo simulation combined with Order Statistics is used for assessing supply reliability. Case studies are performed on a realistic IES that combines an IEEE-15 power system with an 18-node natural gas pipeline network. The efficiency and accuracy of the quasi-steady-state model are validated. The reliability evaluation results show that the inter-correlations among variables and time-dependent relationships of each variable have great effects on the system reliability assessment. The consideration of linepack can significantly improve the supply reliability of IES whereas the management strategy of linepack may lead to some risky points.

**Keywords**: reliability assessment; quasi-steady-state model; CSML model

**Nomenclature**

| | | | |
|---|---|---|---|
| Abbreviations | | $\gamma$ | temperature coefficient |
| CHP | combined heat and power | $\gamma_{\mathrm{G}}$ | specific gravity |
| GPG | Gas-fired power generation | $\varepsilon_{mn}$ | absolute roughness of pipeline *mn* |
| IESs | Integrated Energy Systems | $\eta_{\mathrm{GPG}}$ | energy efficiency of the power plant |
| KDE | Kernel Density Estimation | $\eta_{\mathrm{P2G}}$ | energy efficiency of P2G |
| LBPAM | linepack-based performance analysis model | $\eta_{pv}$ | efficiency of PV |
| OS | Order statistics | $\eta_{\mathrm{s}}$ | efficiency of the compressor |
| P2G | Power to Gas | $\boldsymbol{\Pi}$ | parameter set |
| SS-VTD | steady-state variable transport delay | $\boldsymbol{\Sigma}$ | state set |
| parameters | | $\boldsymbol{\Phi}$ | function set |
| $\boldsymbol{D}$ | data set of gas demand | $\boldsymbol{\Omega}$ | strategy set |
| $D_{mn}$ | diameter of the pipeline *mn* | variables | |
| $E_{\mathrm{p},mn}$ | pipeline efficiency | $C$ | multivariate distribution function which is called copula associated with $H$ |
| $f_{mn}$ | friction factor | $CC$ | cumulative changes |
| $G$, $G_{\mathrm{r}}$ | real and tested solar radiation | $H$ | continuous multivariate cumulative distribution function with uniform marginal distribution functions |
| $g_{ij}$, $b_{ij}$ | conductance and susceptance of nodal admittance matrix, respectively | $C_{mn}$ | hydraulic resistance coefficient of pipeline *mn* |

| | | | |
|---|---|---|---|
| $g_{si}$, $b_{si}$ | conductance and susceptance to ground of node $i$, respectively | $F_p^-$ | generalised quantile functions of $F_p$ |
| $\boldsymbol{I}$ | input set | $F_{r,t}$ | flow rate at time $t$ |
| $IMs$ | individual models | $HP$ | power consumption by the compressor |
| $i$ | number of subsystems | $P_{g,wind}$ | active power of the wind farm |
| $j$ | number of individuals in each subsystem | $P_{ij}$, $Q_{ij}$ | active power and reactive power, respectively |
| $k$ | stage of a hierarchical system | $P_{pv}$ | generated power |
| $k_v$ | specific heat ratio of natural gas | $P_{pv,r}$ | rated capacity of PV |
| $LHV$ | lower heating value of gas | $P_r$ | rated power of wind turbine |
| $\boldsymbol{O}$ | output set | $Q_{d,GPG}$ | gas consumption of GPG for generating power |
| $SMs$ | subsystem models | $Q_{gas,\ mn}$ | gas flow of pipeline $mn$ |
| $\boldsymbol{Sup}$ | a data set of gas supply | $Q_{\mathrm{P2G}}$ | gas consumption of P2G for generating power |
| $T_{\mathrm{b}}$, $P_{\mathrm{b}}$ | gas temperature and pressure at base condition, respectively | $V_r$, $V_{ci}$, $V_{co}$ | rated, cut-in and cut-out wind speeds, respectively |
| $V_k$ | incidence matrix | $Vs_{k,t}$ | inventory capacity in pipeline $k$ |
| $Z_{\mathrm{a}}$ | average compressibility factor | $\Delta demand_{k,t}$ | change of gas demand in the pipeline $k$ from $t$-$1$ to $t$ |

# 1. Introduction

## 1.1 Background

Integrated Energy Systems (IESs), consisting of natural gas pipeline networks, power grids and heating networks, are receiving increasing attention [1-3]. Besides, the term Smart Energy Systems

[4-6] or Sector Integration [7] have sometimes been used to define coherent future sustainable energy systems. In IESs, various types of energy systems can be integrated via different energy conversion technologies, including combined heat and power (CHP) and power to gas (P2G) [8]. The integration can improve renewable energy resources' utilisation efficiency and reduce marginal costs [2]. However, the multi-directional energy flows may present negative effects on the reliability of energy supply if not properly controlled. This is because disturbances in different subsystems can propagate to other systems and affect the whole system's reliability. Various works have focused on the evaluation of the attributes of economy, environment, planning [9] and energy performance [10, 11], but the assessment of reliability for IES is often lacking.

**1.2 Literature review**

For decades, the penetration level of renewable energy resources has been increasing, in support of the energy transition forwards decarbonisation. In IESs, different types of advanced energy conversion technologies have been used. The volatility of renewable resources and the increasingly complex structure of the resulting IESs characterised by multi-scale time dynamics renders complicated the analysis of the reliability of energy supply.

Recently, the issue has been investigated with result to IESs modelling [12] and reliability assessment [13-15]. System reliability assessment methods can be based on probability theory, combined with abstract network theory models, e.g. percolation theory, models of cascading failure [16], and Bayesian networks to capture the conditional degradation among components of the system [17]. However, for complex systems, such as natural gas pipeline networks [18] and power grids [19], abstract topological structures are not sufficient to describe the physical process occurring. Physical models must be associated to simulate and analyse the systems' performance.

The aim of IESs modelling is to assist in the planning of IESs and different perspectives (not only technical but also social and political) may lead to different solutions and decisions [20]. In this work, we have focused on the simulation of system behaviour for reliability assessment to inform the technical side of the planning decision problem.

IESs is a complex hierarchical system, including different subsystems through different kinds of links. The modelling must efficiently describe the complex physical interactions and synergies developing between the different energy resources in the system [1]. Currently, linear steady-state models are widely used. Liu et al. [21] proposed an electrical-hydraulic-thermal steady-state model, which considered the roles of various coupling components, to analyse system performances. Zeng et al. [12] presented a harmonised integration to simulate energy flows in a bi-directional IES, which integrated power systems, natural gas pipeline networks and renewable resources. However, these models ignored the optimisation of energy flows. Then, other literature modelled the optimisation of system operation in linear steady-state models. For example, Wang et al. [22] proposed a linear physical model with simplified optimisation of energy flows to analyse the flexibility of IES. Qadrdan et al. [23] used successive linear programming to deal with the nonlinear problems in the modelling of IES. Lan et al. [24] proposed a state estimation framework for application to gas and electrical systems with equipped low redundancy, based on a steady-state model.

The simplified models neglect the nonlinear characteristics of IESs ensuing from the dynamics and multi-modal behaviours of its subsystems. This deficiency may cause misrepresentations in the results of the analysis and lead to wrong decisions in the system's design and operation. In order to model the nonlinear characteristics of IES, some nonlinear steady-state models have been developed. Devlin et al. [25] combined an economic dispatch model and an energy flow model to investigate the interactions between electric systems and natural gas pipeline networks.

However, these steady-state models, with their simplifications, can lead to deviations in the simulation results from reality, because different subsystems have specific network topologies and characteristics. For example, power systems can reach steady-state within seconds, whereas the hydraulic processes in natural gas pipeline networks last a few minutes [26], the flow dynamics in natural gas pipeline networks depend on the linepack, the volume of gas that can be 'stored' in a gas pipeline and this affects the supply reliability of natural gas pipeline networks.

To analyse the dynamic process in IESs, researchers have developed some models. Generally, based on the nature of each subsystem, steady-state models are used to model power systems. Then, partial differential equations are used to model hydraulic systems. For example, in a multi-time period optimisation model of IESs, Chaudry et al. [27] used partial differential equations to model the transient hydraulic process. The linepack has been considered in natural gas pipeline networks. Fang et al. [28] combined a transient gas model and a DC power model to illustrate dynamic behaviours and simulate different response times of each subsystem. Xu et al. [29] developed a dynamic model, which described natural gas pipeline networks by partial differential equations and described power systems by differential-algebraic equations. This two time-scales dynamic system model can analyse the interactions between subsystems.

Although these physical models improve the realistic description of the characteristics of IESs, the computational burden can be unaffordable for realistically complex systems. Then, quasi-steady-state models have been developed to deal with this problem. On the one hand, some researchers improved traditional methods to model the dynamic process efficiently. For instance, Qin et al. [30] developed a generalised quasi-steady-state IESs model by decomposing the model equations into small parts according to the physical characteristics of IESs. Partial differential equations can be transformed into nonlinear algebraic equations to formulate dynamic thermal systems. The problem of calculating complexity can be overcome. Based on the steady-state heat transfer model, Duquette et al. [31] developed a steady-state variable transport delay (SS-VTD) pipe model, which can describe the dynamic process of heating grids. The steady-state model allowed rapid computation, and the variable transport delay model can describe the hydraulic process. Pan et al. [32] used steady-state models to simulate the dynamic process of electricity and heating systems by dividing the interaction process into four quasi-steady-state stages. The model can describe the interactions between subsystems with time-scale characteristics of IESs. On the other hand, some advanced frameworks have been developed to model heterogeneous complex systems. Wang et al. [33] developed an agent-based model by decoupling heterogeneous complex systems into agents according to physical properties. This model can analyse complex dynamic behaviours with acceptable computational burden.

As mentioned above, various IESs models are used to describe complex systems' behaviours. Steady-state models cannot describe many realistic characteristics of the subsystems of IESs. At the same time, the computational burden of dynamic models is too heavy. Besides, The quasi-steady-state models mainly focus on electric-heat coupling IESs models. An effective and accurate quasi-steady-state electric-gas coupling model is needed for reliability assessment.

Specifically for the reliability assessment of IESs, the need to analyse the influence of uncertainties and disturbances on the response of the specific systems. Thus, the uncertain factors and disturbances must be modelled and their effects integrated with system models. Generally, uncertainties include stochastic energy demands, fluctuations of renewable energy production, system units' failure times, etc. [34]. These factors can be described by probability distributions [35] within multi-state models [36], and the system reliability can be assessed by Monte Carlo techniques

[37]. For example, Kou et al. used two-state models to describe the process of state transition of components and Weibull distributions to define the uncertain power output of wind turbines [38]. Zio et al. [35] used a probabilistic load modelling to describe the intrinsic variability of power load and assessed the system reliability by the Monte Carlo method. Sansavini et al. [39] used probability distributions to describe aleatory uncertainties including demand and wind speed in power systems. The first-order reliability method [14] and the second-order reliability method [40] have also been used to estimate the failure probability of IESs [13, 41, 42].

However, these works used marginal probability distributions to describe the uncertainties of the problem, e.g. related to the energy demand and wind speed, thus neglecting possible dependence relationships between correlated sources of uncertainty [43], e.g. the correlations between energy demands and supplies, the dependence relationships between gas demand and electricity demand. Correlations have been considered in some reliability assessment frameworks. Su et al. [34] used a steady-state IESs model and considered dependent uncertainties within a systematic supply assessment framework. Correlations between energy demands and supplies were formulated by linear and nonlinear methods. Most of the works have not paid sufficient attention to the correlation between uncertain variables like energy consumption and renewable energy production. Generally, different uncertainties are inter-correlated in IESs. This kind of correlation can significantly influence the results of the reliability assessment [44]. The correlation between the stochastic variables describing the uncertainty source should be considered to increase the accuracy and availability of results of reliability assessments. Besides, although some literature has considered the issue, these methods neglected the time-dependent relationships of variables. Because the probability distribution functions of components are the same in different hours. For the steady-state model, the time-dependent relationships can be ignored. However, the time-dependent relationships of variables are quite important in terms of the linepack. Therefore, these models cannot consider the dynamics in reliability assessment [45]. To overcome the problem, time-series data [45-47] have been used in the reliability assessment. However, these methods also cannot consider the correlation between uncertain factors.

On the one hand, the correlation of dependent variables can be modelled by joint probability distributions. For example, Wei et al. [48] proposed a probabilistic method combining the LHS and Nataf transformation. This model used multivariable normal distributions to consider correlations between stochastic natural gas and power demands. Ren et al. [49] used a stochastic response surface method to model multiple correlations between photovoltaic generation, wind power, etc., following normal or non-normal distributions. Uncertainties in IESs usually show nonlinear behaviours and their inter-correlations are naturally complex. Traditional joint distributions such as normal, log-normal, and gamma distributions, require the behaviours of each variable to be characterised by the same parametric group of univariate distributions [50]. The copula approach, which can describe complex dependent relationships between different correlated variables, can avoid this limitation [51]. For example, Fu et al. [52] proposed a copula-based model to describe the dependent structure of dependent generators in distribution networks. This information entropy approach can quantify the uncertainty of IESs effectively. Yu et al. [44] developed a copula-based flexible-stochastic programming method to plan energy systems. The copula function can express dependent relationships between multi-uncertainty sources which have different probability distributions. Mu et al. [53] used a copula function to construct the joint distribution of natural gas price and electricity price, accounting for their correlation.

On the other hand, the time-dependent relationships of system variables can be described by some data-driven methods. Currently, Deep belief networks (DBNs), recurrent neural networks (RNNs), convolutional neural networks (CNNs), Stacked Autoencoders (SAEs), etc. have been proposed to handle high-dimensional data and mine their nonlinear hierarchical features. Therefore, prediction of time-related data such as gas demand and renewable generation [54-56] and system behaviour modelling [45] can be achieved through these data-driven methods. Therefore, in this paper, we used a data-driven method to describe the time-dependent relationships of system variables.

### 1.3 Contributions of this work

(1) Most of the aforementioned works used steady-state models and dynamic models to describe complex systems' behaviours of IESs, whereas quasi-steady-state models were mainly used to model electric-heat coupling systems as shown in Table 1. On the other hand, steady-state models cannot describe realistically all characteristics of the subsystems of IESs, the computational burden of dynamic models of IESs is too heavy, and quasi-steady-state models mainly focus on electric-heat coupling systems. Hence, an effective and accurate quasi-steady-state electric-gas coupling model is needed for reliability assessment.

Table 1 IES modelling

| | IES model | Subsystems | Limitations |
|---|---|---|---|
| Liu et al. [21] | Steady-state | Electricity-heating network | Results are inaccurate as simplifications of network topologies and dynamic characteristics of different subsystems. |
| Zeng et al. [12], Qadrdan et al. [23], Devlin et al. [25] | Steady-state | Electricity-natural gas networks | Results are inaccurate due to simplifications of network topologies and dynamic characteristics of different subsystems. |
| Chaudry et al. [27], Fang et al. [28], Xu et al. [29] | Dynamic | Electricity-natural gas networks | The computational burden of the dynamic models is too heavy. |
| Qin et al. [30], Pan et al. [32], Wang et al. [33] | Quasi-steady-state | Electricity-heating network | Main focus on electric-heat coupling systems. |

(2) Since the aforementioned models ignore the inter-relationships among uncertain factors and the time-dependent relationships in the uncertainty modelling for reliability assessment, as represented in Table 2, it is necessary to provide a framework to allow accounting for the inter-relationships and the time-dependent relationships of the system variables, because these relationships are important in the reliability assessment.

Table 2 Uncertainty modelling

| | Inter-relationships | Time-dependent relationships | Methods |
|---|---|---|---|
| Zio et al. [35], Sansavini et al. [39] | Ignored | Ignored | Marginal probability distributions |
| Su et al. [34] | Considered | Ignored | Linear and nonlinear methods |

| | | | |
|---|---|---|---|
| References [45-47] | Ignored | Considered | Time-series |

To deal with such research gaps, we propose a systematic framework of the reliability assessment of IES. Firstly, a novel unified quasi-steady-state IES model is developed for the dynamic state analysis of IES with bi-directional energy conversion. The operational strategies of linepack utilisation are considered to meet the requirement of the contract pressure. Then, the correlations between different uncertain factors and the time-dependent relationships of system variables are considered by a statistics-machine learning-based model. A first case (Case 1) is conducted to demonstrate the feasibility of the proposed quasi-steady-state model. In Case 2, the efficiency of the statistics-machine learning-based method is studied and the influence of the available linepack on the reliability of IESs is investigated by the proposed framework in Case 3.

The main contributions in the paper can be summarised as:

(1) A unified quasi-steady-state electric-gas IES model with bi-directional energy conversion is proposed based on the linepack-based performance analysis method (LBPAM). LBPAM can consider pipelines' storage capacity and operational strategies, based on linepack for natural gas pipeline networks.

(2) A model that combines the statistical structure of empirical copula with the machine learning method of the stacked autoencoder is developed. The correlations between different uncertain factors and the time-dependent relationships of system variables are considered in the model.

(3) A reliability assessment framework is proposed for IES. The quasi-steady-state model, statistics-machine learning-based model and OS (Order statistics) are combined in the framework. Based on the framework, dynamic reliability can be analysed by using the sampled time series data. The influence of the available linepack, the requirement of contract pressure and the management strategy of linepack on the reliability of IESs are investigated. The results allow investigating the impact of linepack on practical operations for supply reliability.

The remainder of this paper is organised as follows: Section 2 describes the quasi-steady-state IES model and the definition of the empirical copula and OS. In Section 3, realistic cases are simulated to verify the effectiveness of the proposed methods. Section 4 gives the conclusions of the work.

## 2 Methodology

The framework for the supply reliability assessment includes IESs modelling and reliability evaluation. Firstly, based on the linepack-based performance analysis method (LBPAM), a unified quasi-steady-state IES model with bi-directional energy conversion is developed in such a way to take into account the multi-modal characteristics in IES especially the nature of linepack in natural gas pipeline networks. Secondly, the CSML method is used to structure the relationships between uncertainty factors, and the time-dependent relationships of each variable. Then, the Monte Carlo technique combined with Order Statistics is used to assess the supply reliability of the IESs, with reduced computational burden.

The formulations of the AC power flow model, basic natural gas pipeline networks model, energy conversion modelling and renewables generation models are described in Appendix A.

### 2.1 Systematic modelling of IESs

Based on the steady-state IES model [41], the quasi-steady-state model is established combined with the linepack-based performance analysis method. In this model, we neglect the transient nature of power systems because they can reach steady-state within seconds. A unified formulation for the steady-state analysis of IES [12] is the basis of the physical model. Then, the LBPAM is used to improve the performance analysis of natural gas pipeline networks so that the dynamics can be considered in the model.

In this work, IES includes electric power systems, natural gas pipeline networks, renewable resources productions, gas compressors, the power-to-gas and gas-fired power plants.

### 2.2 Framework of the developed Linepack-based performance analysis method

The linepack-based performance analysis method (LBPAM) is described in this subsection and its application for the analysis of IESs.

The flowchart of the quasi-steady-state is shown in Fig. 1.

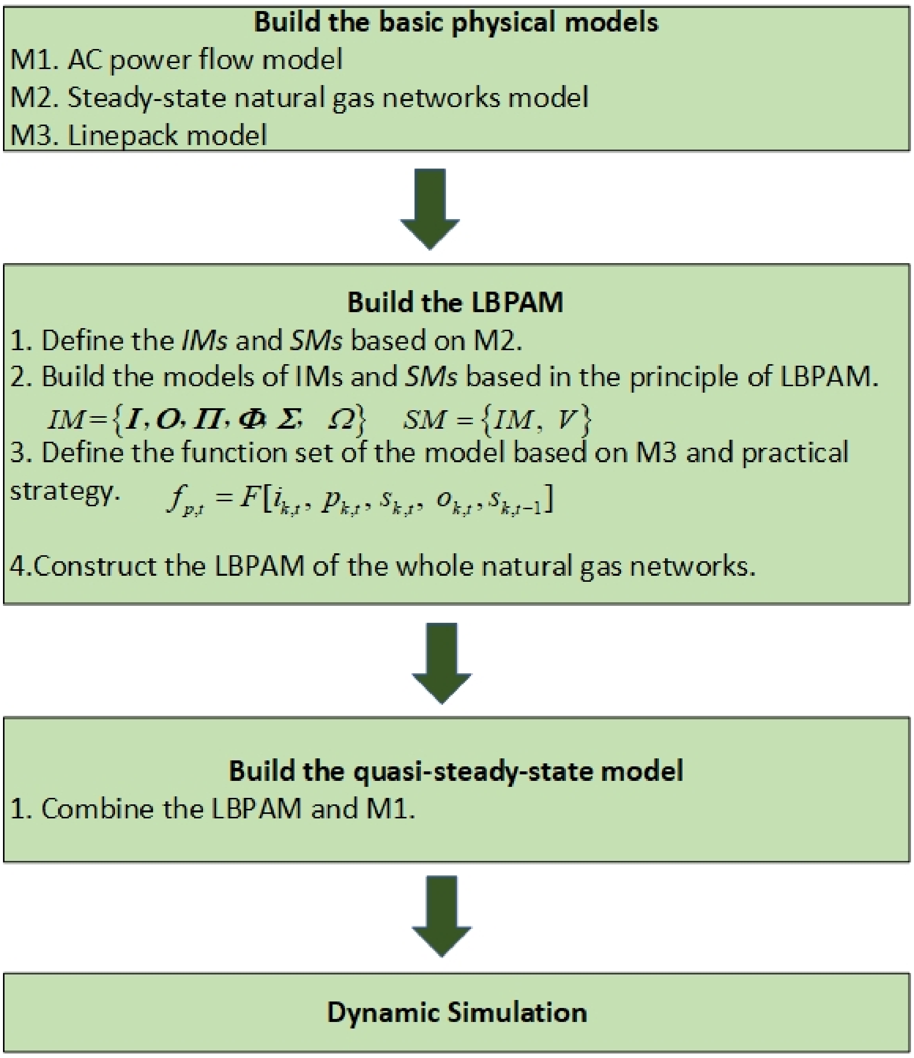


Fig. 1. Flowchart of the quasi-steady-state model

Firstly, a physical model of an IES is used, which combines natural gas pipeline networks and power grids. The basic physical models are established including the AC model for the electricity system, the steady-state model and linepack model for natural gas pipeline networks. Then, the individual models (IMs) and subsystem models (SMs) are defined according to the natural gas pipeline networks model and the principle of LBPAM. The steps of the LBPAM is shown as follows (the structure is shown in Fig. 2). (1) Build the IMs and SMs. All pipelines are indicated by $\{IM_1, IM_2, \ldots IM_j\}$. Subsystems (or transmission pipelines) that include some pipelines in a specific zone are indicated as $\{SM^1_1, SM^1_2, \ldots SM^1_k, SM^2_1, SM^2_2, \ldots SM^2_k, \ldots, SM^k_k\}$. (2) Define the function set based on the linepack model and some practical strategies. (3) Integrate the LBPAM and AC power flow model to form the quasi-steady-state model. An initial condition is predefined so as to obtain the initial inventory (the initial natural gas stored in a specific pipeline) and system state. Input parameters are set according to the time series of load demands, renewables generations, gas supply, etc. Then, the state of all IMs and SMs can be developed by the principles of LBPAM and the data information can be transferred to the next time step. Therefore, the dynamic behaviours of IESs can be calculated by updating the states of each iteration in time.

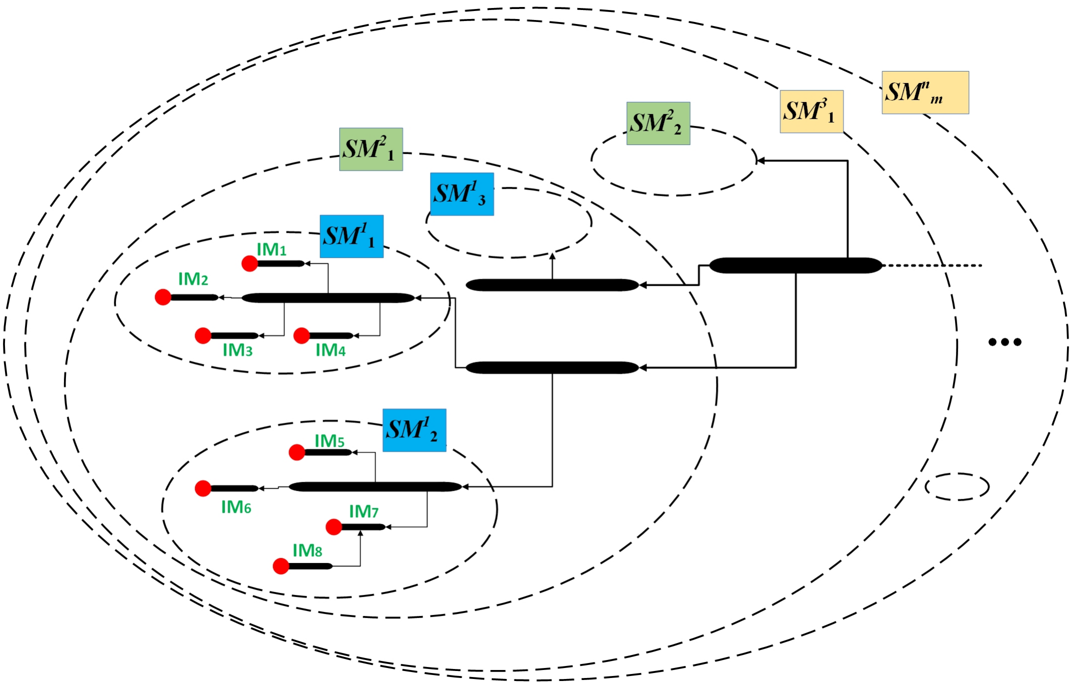


Fig. 2. The structure of a simple hierarchical system

**2.2.1 Definition of LBPAM**

In order to categorise different layer objects effectively, the LBPAM consists of *IM* individual models and *SM* subsystem model. *IM* represents a single pipeline; *SM* represents the subsystem, including some pipelines or smaller subsystems in a specific area. Several individual elements can make up a subsystem, and several small subsystems can make up a bigger subsystem. The proposed LBPAM is composed of several layered objects; a simple structure of the hierarchical system is shown in Fig. 2.

As shown in Fig. 2, natural gas pipeline networks can be described by some subsystems and elements. Each pipeline has individual inherent characteristics and parameters, such as lengths and diameters. The mathematical representation of the subsystem model is given by (Eq. 1):

$$
\begin{aligned}
SM_{i1,t}^{1} &= \left\{ IM_{j,t}^{0},\ V_{1} \right\} \\
SM_{i2,t}^{2} &= \left\{ SM_{i1,t}^{1},\ V_{2} \right\} \\
&\vdots \\
SM_{ik,t}^{k} &= \left\{ SM_{i(k-1),t}^{k-1},\ V_{k} \right\}
\end{aligned} \tag{1}
$$

where $j$ is the number of individuals in each subsystem; $k$ is the stage of the hierarchical system; $i1$, $i2$, ..., $ik$ represent the number of subsystems at each hierarchy, respectively; $V_k$ is the incidence matrix to the connections between different elements and between subsystems.

Each *IM* and *SM* can be described mathematically as (Eq. 2):

$$IM = \left\{ \boldsymbol{I}, \boldsymbol{O}, \boldsymbol{\Pi}, \boldsymbol{\Phi}, \boldsymbol{\Sigma},\ \Omega \right\} \tag{2}$$

where *IM* is a six-tuple of the input set ($\boldsymbol{I}$), the output set ($\boldsymbol{O}$), the parameter set ($\boldsymbol{\Pi}$), the function set ($\boldsymbol{\Phi}$), the state set ($\boldsymbol{\Sigma}$), and the strategy set ($\Omega$).

The input matrix $\boldsymbol{I}$ is composed of the gas demand $d_{k,\,t}$ and the gas supply $sup_{k,\,t}$ at time $t$ of each node $k$ and the state $s_{k,\,t-1}$ at time $t$-1 of pipeline $k$. Assuming $\boldsymbol{D}$ is a data set of gas demand and $\boldsymbol{Sup}$ is a data set of gas supply, the input $i_{k,\,t}$ can be given as (Eq. 3):

$$i_{k,t} = \left\{ \left( d_{k,t},\ s_{k,t-1},\ \ sup_{k,t} \right) \middle| d_{k,t} \in \boldsymbol{D},\ sup_{k,t} \in \boldsymbol{Sup},\ k \in \boldsymbol{K},\ t \in \boldsymbol{T} \right\} \tag{3}$$

where $s_{k,\,t}$ represents the state of pipeline $k$ of time $t$, and it affects the decision-making on the operation of the system. The inventory of a pipeline is part of $s_{k,\,t-1}$, which determines whether the gas stored in the pipeline is enough for the demand of the next time step $t$ (Eq. 4).

$$\boldsymbol{\Sigma} = \left\{ s_{k,t} \middle| k \in \boldsymbol{K},\ t \in \boldsymbol{T} \right\} \tag{4}$$

$O_{k,\,t}$ is the output of each element at time $t$, which can be described as (Eq. 5):

$$\boldsymbol{O} = \left\{ o_{k,t} \middle| k \in \boldsymbol{K},\ t \in \boldsymbol{T} \right\} \tag{5}$$

The overall output, such as the system's functional state and delivery pressures, is updated at each time step during the simulation.

The inherent characteristics of the elements $\boldsymbol{\Pi}$, described by given parameters $p$, change as a function of time $t$. The mathematical description of $\boldsymbol{\Pi}$ is defined as (Eq. 6):

$$\boldsymbol{\Pi} = \left\{ p_{k,t} \middle| k \in \boldsymbol{K},\ t \in \boldsymbol{T} \right\} \tag{6}$$

Physically-based equations and rules in the function set are essential to describe the whole process. Depending on $i_{k,\,t}$, $s_{k,\,t}$, and $p_{k,\,t}$, the function set, which describes the physical mechanism of an element, maps { $i_{k,t}$, $s_{k,t-1}$, $p_{k,t}$ } to {$s_{k,t}$, $o_{p,t}$ }, as given in Eq. 7:

$$f_{p,t} = F[i_{k,t},\ p_{k,t},\ s_{k,t},\ o_{k,t}, s_{k,t-1}] \tag{7}$$

It should be noted that the operational strategies ($\Omega$) in this model make full use of the linepack explicit formulation, determining the valve opening of each station for gas supply. Based on variables, such as the capacity of the linepack of each natural gas pipeline and gas demand, $\Omega$ can be expressed as (Eq. 8):

$$\begin{aligned}
&\Omega = F[i_{k,t}, s_{k,t-1}] \\
&\text{Example:} \\
&(1)\ demand_{k,t} \geq demand_{k,t-1}: \\
&\text{if } Vs_{k,t-1} \geq \Delta demand_{k,t}\ \&\ (Vs_{k,t-1} - \Delta demand_{k,t}) \geq Vs_{p,\min} \\
&Vs_{k,t} = Vs_{k,t-1} - \Delta demand_{k,t} \\
&\text{else } Vs_{k,t} = F[i_{k,t},\ p_{k,t}] \\
&(2)\ demand_{k,t} < demand_{k,t-1}: \\
&\text{if } (Vs_{k,t-1} + \Delta demand_{k,t}) \leq Vs_{p,\max} \\
&Vs_{k,t} = Vs_{k,t-1} + \Delta demand_{k,t} \\
&\text{else } Vs_{k,t} = F[i_{k,t},\ p_{k,t}]
\end{aligned} \tag{8}$$

where $\Delta demand_{k,t}$ is the change of gas demand in the pipeline $k$ from $t$-1 to $t$; $Vs_{k,t}$, $Vs_{p,\min}$ and $Vs_{p,\max}$ are the inventory, minimum inventory and maximum inventory capacities in pipeline $k$, respectively.

**2.3 The CSML model**

The CSML model, which can sample time-series data of variables, is proposed based on the empirical copula and stacked auto-encoder model. The empirical copula is used to establish the joint probability distribution of uncertainties whereas the stacked auto-encoder model can model the time-dependent relationships of each system variable. The realisations sampled by the empirical copula at time $t$ and the realisations sampled at time $t$+1 are related, and this relationship can be established by the stacked auto-encoder model. The simple structure is shown in Fig. 3.

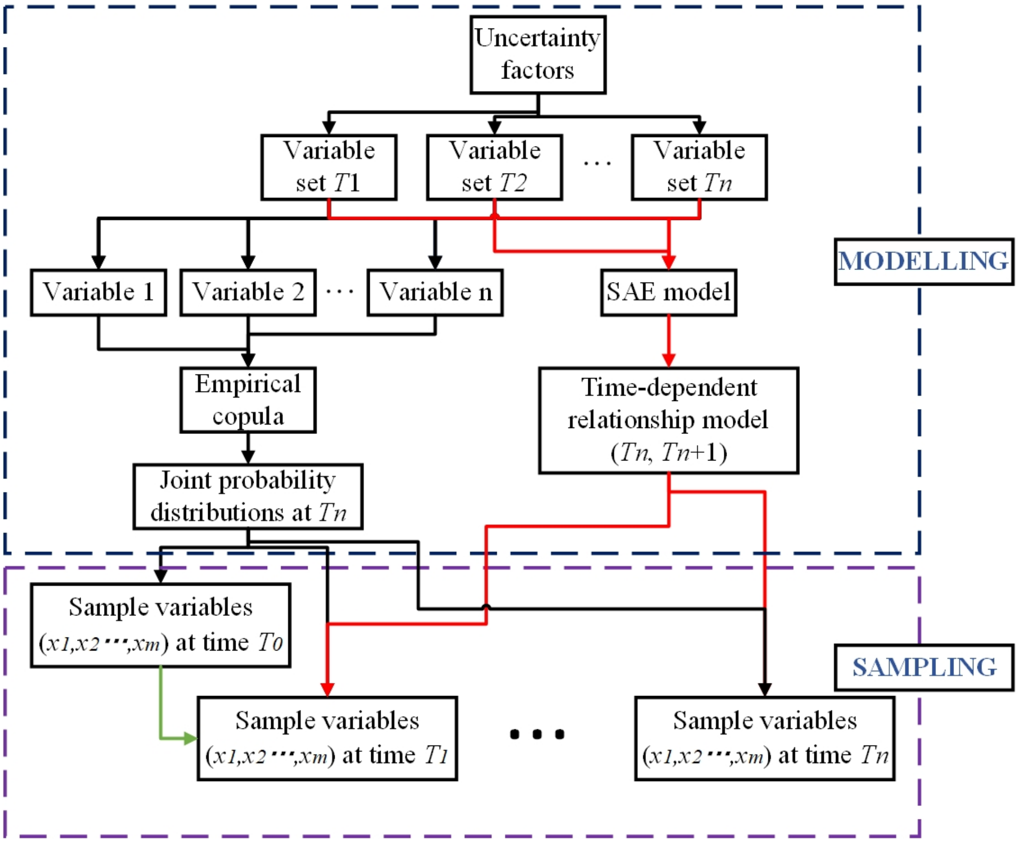


Fig. 3 The structure of the CSML model

The formulations of the empirical copula and SAE model are shown in Appendix B.

**2.3.1 Static scenario generation based on empirical copula function**

In this work, we consider the relationships between natural gas demand $Gd_t$ and electricity demand $Ed_t$. Considering random variables $Gd_t$ and $Ed_t$ that follow $\Pr(Gd_t \le p_G) = F_G(p_G)$ and $\Pr(Ed_t \le p_E) = F_E(p_E)$, respectively, the joint distribution function of the two random variables is named $\Pr(Gd_t \le p_G, Ed_t \le p_E) = C(p_G, p_E)$, where $C$ is the empirical copula function. The gas demand and electricity demand at time t are generated by:

$$\begin{cases} (Gd_t, Ed_t) = C^{-1}(U_G, U_E) \\ [U_G, U_E] \sim U_{G,\mathrm{nif}}[0,1] \times U_{E,\mathrm{nif}}[0,1] \end{cases} \tag{9}$$

where $U_{\mathrm{nif}}[0,1]$ is the uniform distribution in [0,1]; $C$ presents the empirical copula function. The marginal distributions of random variables are presented as:

$$\begin{cases} Gd_t = F_G^{-1}(U_G) \\ Ed_t = F_E^{-1}(U_E) \end{cases} \tag{10}$$

As the historical data of random variables, e.g. natural gas demand and electricity demand, are fitted to obtain the joint distribution empirical copula function, the empirical copula function is discretized to generate the static scenario generation at time t based on Eq. 10 and Eq. B6.

### 2.3.2 Time series data generation based on the SAE model

As the static scenarios are generated by empirical copula functions, the time series data is generated in the combination of the SAE model.

Given that the static scenarios are generated by empirical copula functions, the time series data is ,then, generated by combination with the SAE model.

First, to model the stochasticity of the variables, we use the SAE model to mine from historical data the internal relationships of the time series data of the variables across time steps. We assume a multivariate random vector $De=[De_1, De_2, \ldots, De_m]^T$, where m is the time span. The correlation between $De_i$ and $De_j$ is characterized by the SAE model. Then, as the static scenarios *[Det]* are generated at time t, [*Det*] is input into the SAE model to get a reference scenario [$De^*_{t+1}$] at time $t$+1. Comparing the reference scenario and the scenario sampled by means of the empirical copula functions and calculating the different value Δ* of them, If $\Delta^* \le \varepsilon^* (\varepsilon^* = 1\times 10^{-4})$, the generated scenario is retained. Otherwise, re-sampling of the scenario by the empirical copula functions is performed until the data meet the requirement. Then, the procedure moves to the next time step and by continuing the time series data is generated.

## 3 Case studies

In this section, a realistic IES is used to verify the validity and effectiveness of the proposed systematic framework for supply reliability assessment. A bi-directional steady-state IES model, a dynamic IES model and a quasi-steady-state IES model based on LBPAM are developed to analyse the performance of the IES. The basic structure of the IES is shown in Fig. 3.

The uncertainties in our model can be divided into two categories in relation to physical parameters and scenario parameters. For example, the electricity demand and gas demand are uncertain scenario parameters; the uncertain physical parameters are related to physical properties of materials, such as the density and heat capacity of walls, etc.

In this work, a model that combines the statistical structure of uncertain parameters with a machine learning method is developed to define the time multivariate joint distributions for variables. For the application to IES, electricity demand and natural gas demand are most relevant uncertainties, to which, we paid most attention. We also considered the failure probabilities of components in the reliability assessment, e.g. compressor stations and gas-fired power generation stations. The failure probabilities of the components are taken from Ref. [45]

In this work, an IES model combining an IEEE-15 power system with an 18-node natural gas pipeline network is considered to validate the proposed method, as shown in Fig. 4. The AC power flow model is used to simulate the behaviour of grids ( the related formulas are given in Appendix). Based on the unified energy flow formulation [12], the quasi-steady-state model of the natural gas and electric power system is obtained by combining the linepack-based performance analyses model and AC power flow model through links of the gas compressor, P2G and gas-fired power plants. The model allows describing the nodal balance and branch flow in IESs. Different from dynamic models, energy dispatch calculations are solved with the Newton–Raphson method in quasi-steady-state simulation but the natural gas characteristics are taken into account. In our case, gas-fired generators, gas compressors and P2G are the links considered to connect the two systems. The interdependent data, e.g. gas consumption of gas-fired generators and gas compressors, and electricity consumption of P2G, are exchanged during the solution process.

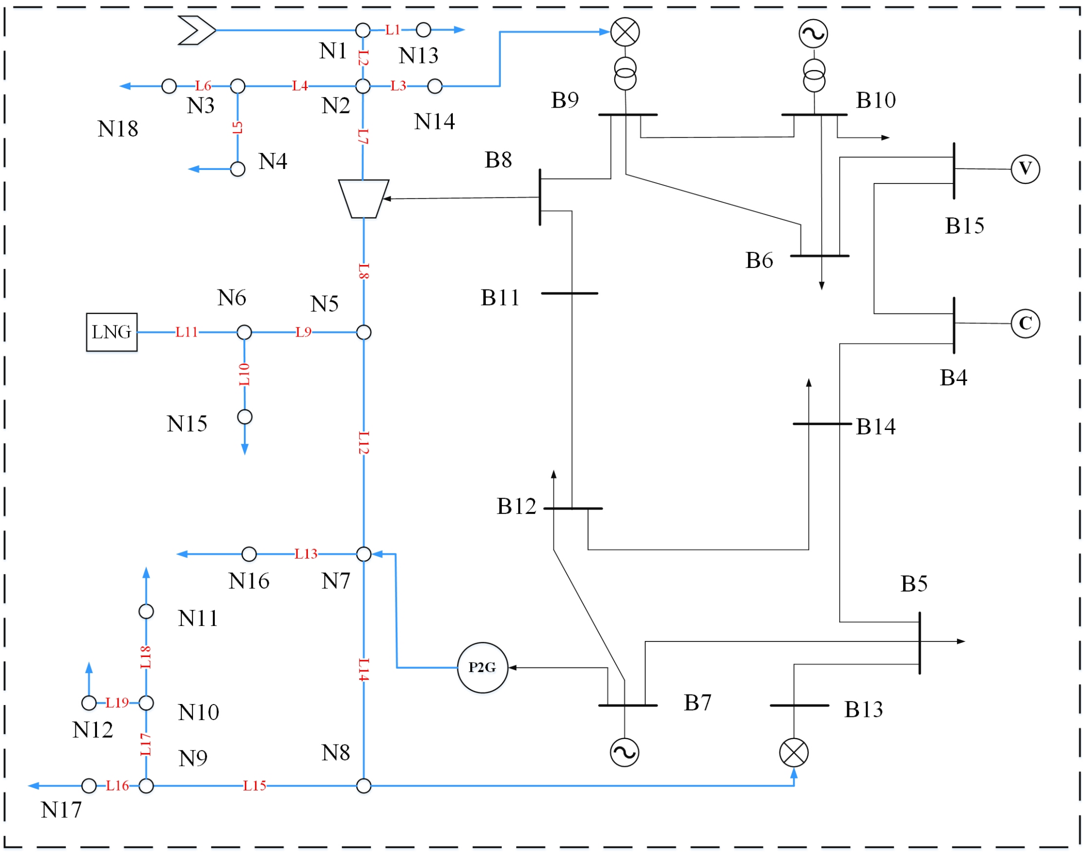


Fig. 4. Structure of the IES

The natural gas pipeline network is decomposed into several *IM*s and *SM*s. Different *IM*s and *SM*s can exchange information. In one time step, *IM*s are developed firstly; then, the results from *IM*s convert to *SM*s. As the whole process of LBPAM is finished, the simulation of the IES model at time $t$ is completed. The results can be used to evaluate the performance of the IES at time $t$+1. At time $t$+1, the simulation proceeds, and the results at time $t$ are converted to the time step $t$+1.

As shown in Fig. 4, there are nine basic individuals (L1, L3, L5, L6, L10, L13, L16, L18, L19) and several subsystems. For instance, L17, L18 and L19 make up a subsystem.

The initial state is at step 0 and the LBPAM has the original inventory of each pipeline. Then, at step 1, the changes in demand and supply of energy at N11 occur. Because these disturbances can affect the performance of IESs according to the principle of LBPAM, if the linepack capacity of the natural gas pipeline network can handle these disturbances within its scope in L18, the gas supply from N10 will not change for maintaining the operation stability. Suppose the linepack capacity of L18 cannot deal with these disturbances.The linepack of L17, the upstream of L18, will be considered to compensate for surplus load demand at N11. Then, the dynamic process can be effectively described through the changes of linepack.

A number of case studies were undertaken. In Case 1, simulation results from a traditional bi-directional steady-state IES model, a dynamic model and the proposed quasi-steady-state model are analysed. In Case 2, supply reliability is analysed based on the proposed framework, to highlight the importance of accounting for the inter-correlations between uncertainty factors. In case 3, the effect of linepack in the IES is investigated.

## 4 Simulation and results

### 4.1 Case1: Comparison among IES models

#### A. Discussion on the flow rate fluctuation

As gas and power demands vary with time, terminal stations need to adjust the gas supply to maintain the customers' demands. As shown in Fig. 4 and Fig. 5, the flow rate of gas supply from upstream stations changes with time in different models. It can be observed that the frequency of changes in flow rates is lower in the proposed IES modelling framework than that in the steady-state model. In the steady-state model, the gas supply from upstream must change every hour to satisfy the gas load variation (the mass flow rate changes every hour). However, the flow rate fluctuation from upstream can be reduced when the linepack and the related strategies are considered, like in the proposed model, as shown in Fig. 5. This allows the flow rate to be kept unchanged in some time intervals, to keep the stability of the IES. For example, the black line in Fig. 5 represents the gas supply from station N1 to pipeline L1. The flow rate (gas supply) has to change every hour to deal with the varying gas loads during the entire period in the steady-state model. In contrast, the flow rate can be kept constant within hours 4-9 and hours 9-23 in the quasi-steady-state model.

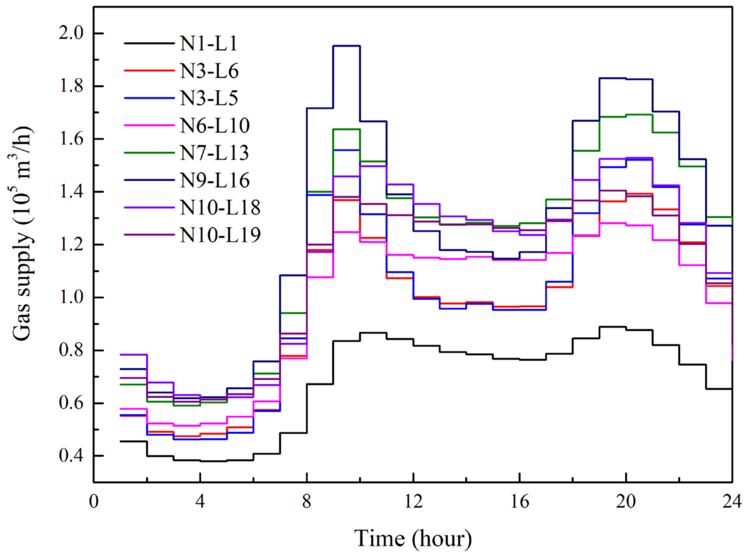


Fig. 5(a). The gas supply from inlets node in the steady-state IES model

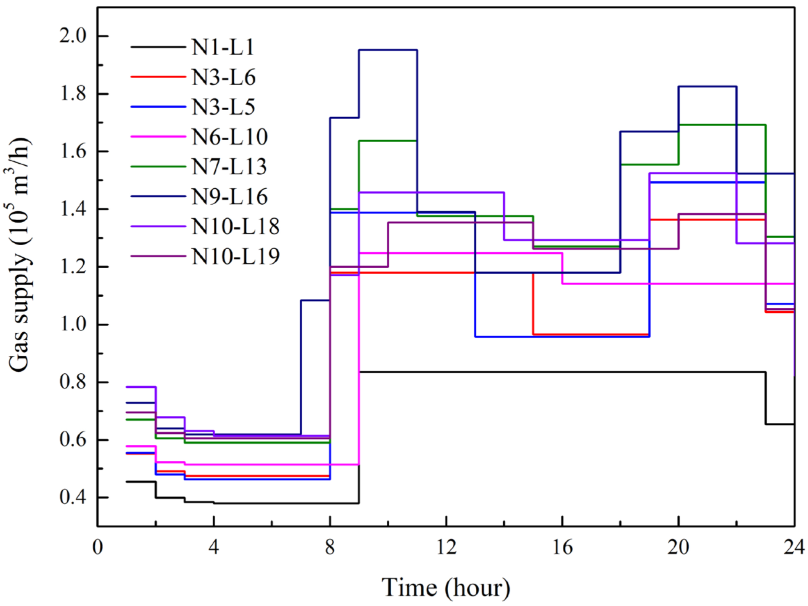


Fig. 5(b). The gas supply from inlet nodes in the proposed IES model

To illustrate the volatility of flow rates quantitatively in the two models, standard deviation and cumulative changes (*CC*) (Eq. 28) during the period in each pipeline are calculated, and shown in Fig. 6:

$$CC = \sum_{t=1}^{T_p} \left| F_{r,t} - F_{r,t-1} \right| \tag{9}$$

where $F_{r,t}$ is the flow rate at time $t$ and $CC$ is the value of cumulative changes.

As shown in Fig. 6, the standard deviation of the flow rate (the bars in the figure) in the proposed model is lower in almost all pipelines than that of the steady-state model. However, the results in other pipelines are different, such as for pipeline L1. This is because the standard deviation value only indicates how close the values are to the average value of the sample set. It cannot describe the stability of the data. Therefore, $CC$ is defined as a complementary index to further assess the volatility of flow rates. Indeed, all values of $CC$ are higher in the steady-state model, indicating frequent fluctuations in flow rates.

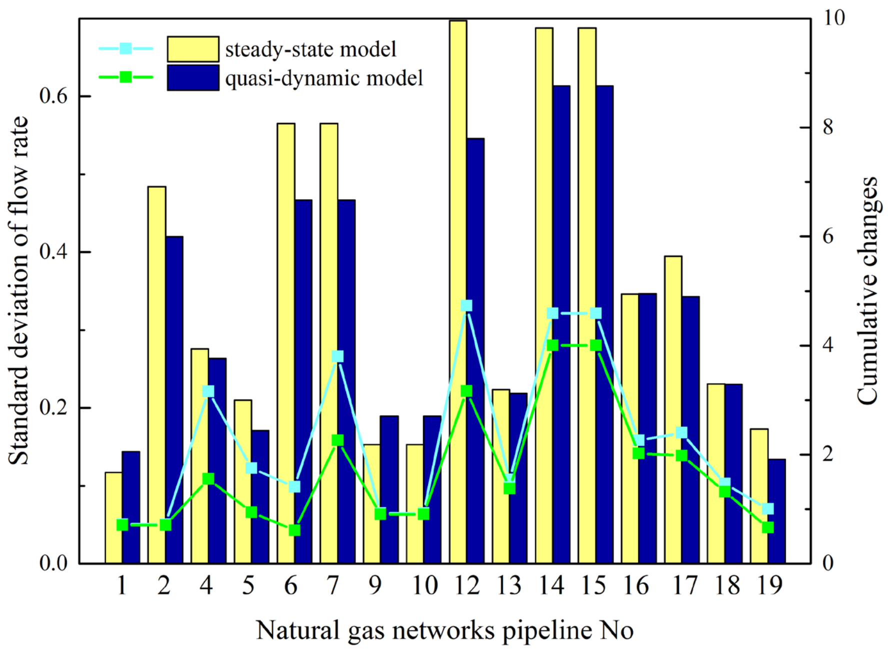


Fig. 6. Standard deviation and cumulative changes of flow rates in each pipeline

The fluctuation of flow rates in the steady-state model is more frequent than that of the proposed model because the steady-state model ignores the storage capability of natural gas pipeline networks. This allows that neglecting the storage capability of pipelines may lead to erroneous results.

In the above cases, the time step is 1 hour. If the time step becomes smaller, such as 1 minute or even 1 second, the fluctuation of gas supply in the steady-state model will be even more frequent.

It may lead to requiring operators to adjust valves according to the time step, which is infeasible in practice. On the contrary, in the proposed model, the fluctuation of gas supply can remain unchanged for a long time even though the time step is 1 hour. The reason is that the linepack can keep the balance between demand and supply, under gas demand changes within an acceptable range. The system operational stability can be guaranteed.

The dynamic models of natural gas pipeline networks can also describe the nature of linepack. We compare the proposed model and the dynamic model [28] in terms of the description of the linepack. The gas supply from N10 and the available linepack at L18 are shown in Fig. 7. In the dynamic models, the flow rate changes with the changes of demand. The changes in flow rates have a delay due to the compressibility of natural gas. This leads to changes in linepack that are different in some periods (hours 6-11). It should be noted that the available linepack in the dynamic model goes below zero at hours 19-24. The reason is that the model does not consider the constrictions of delivery pressure (the contract pressure). The proposed model, instead, can consider minimal contract pressure in the operational strategies set ($\Omega$).

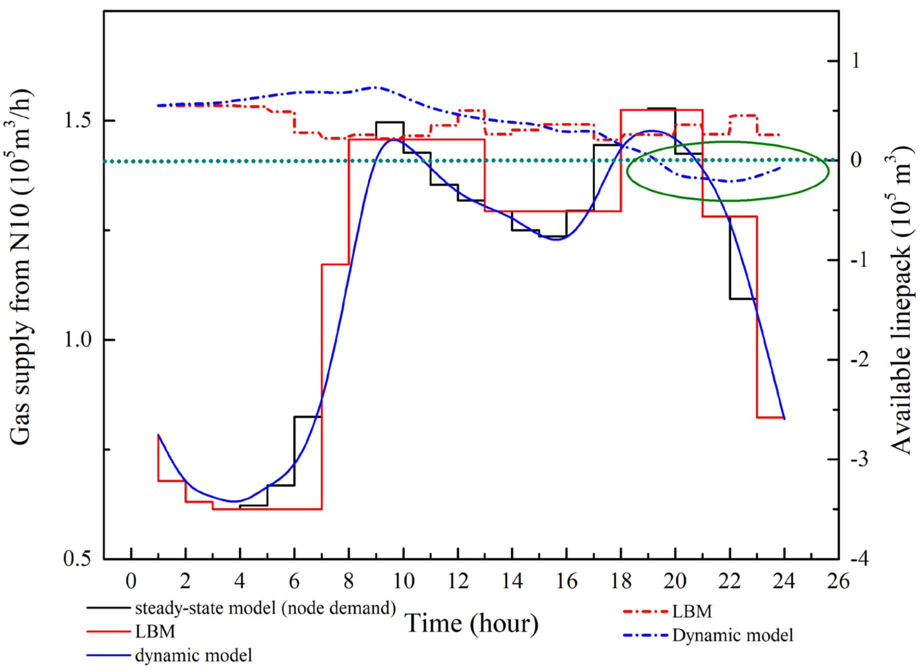


Fig. 7. Gas supply from N10 and available linepack at L18

**B. Discussion on the accuracy for reliability assessment**

As shown in Fig. 8, the simulation results derived from different models are different, although the input parameters are the same. In hours 7, 19 and 20, the balance between energy demand and energy supply can be kept by the quasi-steady-state model. In contrast, the traditional steady-state model cannot guarantee the reliability of supply. There is no difference between flow rates at the outlet and inlet of a pipeline in the steady-state model. Thus, the system will be regarded as failed once the gas supply is less than the gas demand at any time step. However, natural gas stored in pipelines can provide surplus natural gas to satisfy increased demand to a certain extent as accounted for in the proposed model.

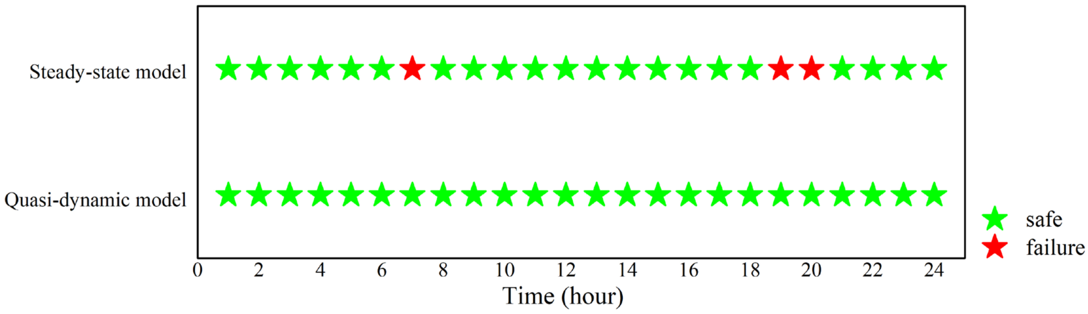


Fig. 8. Simulation results in different models

In practice, gas supply from gas stations only changes once or twice per day. Small changes in gas demand can be handled by the linepack generally. Fig. 9 presents the changes of linepack in the quasi-steady-state model. The value of linepack changes in response to gas demand changes. As shown in Fig. 9, the tendency of the linepack is opposite to the trend of gas demand, precisely for mitigating the demand fluctuation. The increase of gas demand depletes natural gas stored in pipelines to ensure supply reliability, resulting in the reduction of the linepack. On the contrary, the reduction of gas demand leads to the surplus gas provided from upstream being stored in pipelines, and the linepack rises.

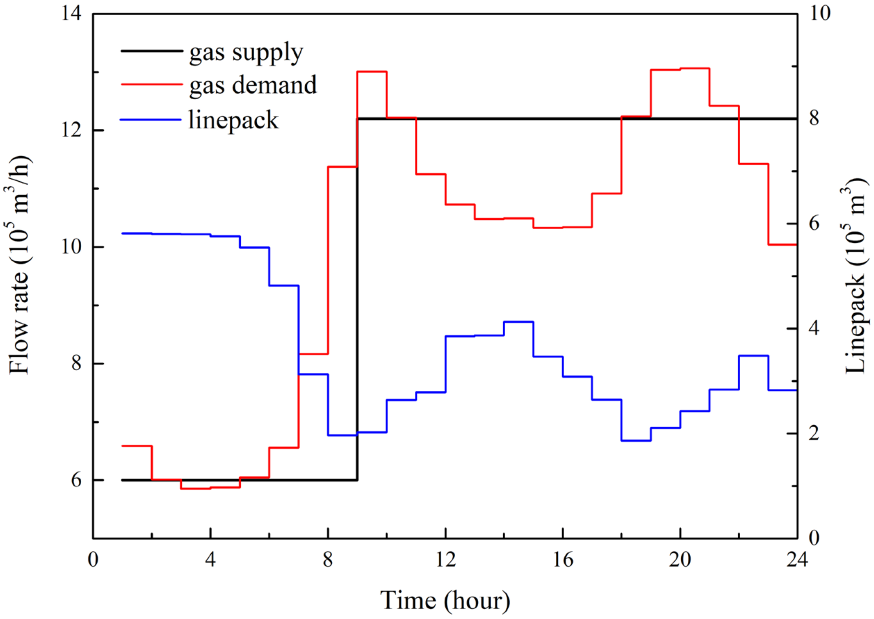


Fig. 9. Gas supply, gas demand and linepack during the period of one day

In summary, using the LBPAM allows realistically describing the dynamic behaviour of IES, especially concerning the linepack effects in natural gas pipeline networks. The quasi-steady-state process allows analysing the dynamic behaviours of IESs, while the computational burden remains the same as that of the steady-state model. The linepack allows considering that the volume of gas injected into pipelines can be higher than the volume of natural gas withdrawn from upstream, and the surplus natural gas can be temporarily stored in the pipelines; then, natural gas supply can be provided in peak demand hours avoiding natural gas shortage. By accounting for this, the quasi-steady-state can improve the accuracy of the supply reliability assessment of IES.

**4.2 Case 2: The impacts of the relationships between uncertainties**

In this case, to analyse the impacts of the relationships between the uncertain power and natural gas demands and the time-dependent relationships of system variables on the reliability assessment. KED and the CSML method are used.

KED can provide the independent probability distribution functions of power demand and natural gas demand at each hour. For the CSML method, the empirical copula is, then, used to estimate the joint distribution, describing the inter-dependence structures existing between power demand and natural gas demand. The time-dependent relationships of the uncertain variables are constructed by an SAE model.

The Pearson correlation coefficients between power demand and natural gas demand, Pearson correlation coefficients between different continuous hours and failure probabilities of the IES in different scenarios are shown in Fig. 10. The correlation coefficients between different continuous hours are higher than 0.86. It means the degrees of variables between continuous hours have strong interdependences. As shown in Fig. 10 (C), the system can be 100% safe excluding hour 7. The reason is that the time-dependent relationships between $T$ and $T$+1 are neglected. Therefore, the sample data can be different in each scenario. In the steady-state model, the impact of the value of variables at hour $T$ can be ignored at hour $T$+$n$. However, in the dynamic simulation, the effects are very important in terms of the change of linepack. That is why the profiles of reliability in different scenarios are quite distinct (Fig. 10 (C)).

The reliability in hours 1-5 and hours 11-17 are the same in two scenarios when the energy demands are relatively low. This is because the energy supply is sufficient to satisfy energy demand. The inter-relations and time-dependent effects can be neglected in this circumstance (correlation coefficients between demands are lower than 0.5). However, when demands increase sharply, reliability becomes different in different scenarios. In hour 7, the failure probability is lower as the correlations between power demand and natural gas demand are considered (the correlation coefficient is higher than 0.8). In hours 18-23, the value of reliability can be 1 when the probability distributions of different demands are estimated by KDE separately. On the contrary, the system is shown to suffer energy shortage when the proposed model is used to construct the joint distribution of different energy demands (correlation coefficients are higher than 0.5 at hours 18-21). Although correlation coefficients are lower than 0.5 at hours 22-23, the depletion of the linepack at hours 18-21 may increase the probability of energy shortage at hours 22-23.

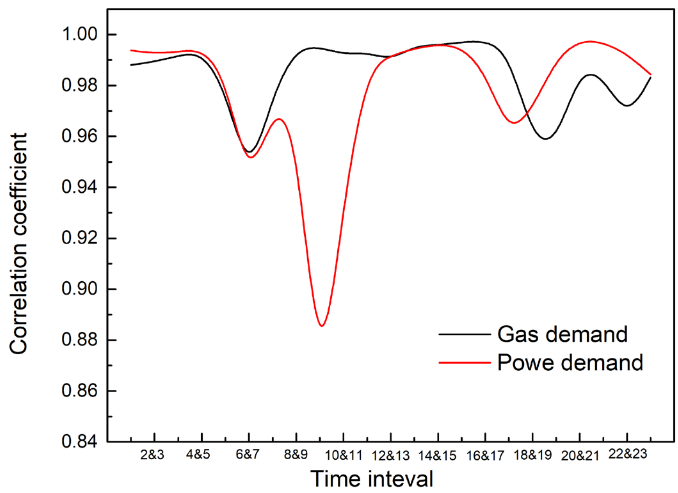


(A) Pearson correlation coefficients of variables between different hours

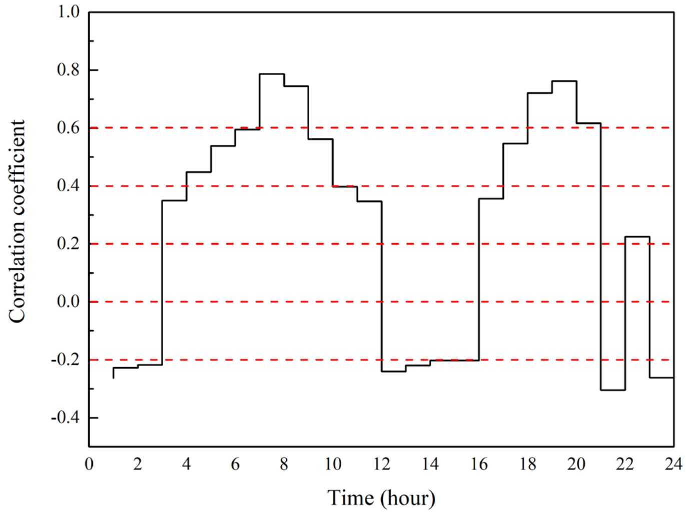


(B) Pearson correlation coefficients between power demand and natural gas demand

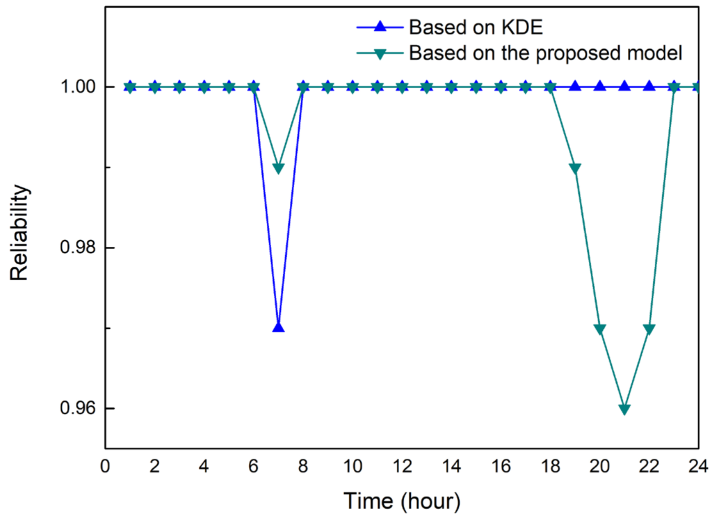


(C) Reliability of the IES under different scenarios

Fig. 10. The Pearson correlation coefficients and reliability of the IES

**4.3 Case 3: The importance of linepack and the management strategy of linepack**

In this case, the importance of linepack and the management strategy of linepack are investigated, considering the requirement of contract pressure. The management strategy of the linepack is shown in Eq. 8.

In order to investigate the impact of contract pressure (the minimal pressure at the outlet), we considered $a \cdot P_{2\min}$ as the contract pressure, with $a$ being a parameter with values in the range (0.5-1.1), instead of the original contract pressure $P_{2\min}$. The lowest values of reliability with 95% confidence in different scenarios ($a$ takes different values) are shown in Fig. 12. In most hours, the reliability of the system increases with the reduction of the contract pressure (a<1). It shows that the increase of available linepack can improve the reliability of the IES. However, at hour 7, the reliability decreases with reduced contract pressure. This result is opposite to that of other times. The available linepack is sufficient to satisfy natural gas demand increase at hours 1-6 and the natural gas supply from upstream keeps unchanged. But, the available linepack reduction at hours 1-6 leads to having insufficient available linepack at hour 7. Then, when natural gas demand increases dramatically at hour 7, the failure probability increases. As shown in Fig. 13, the min and max values of reliability in different scenarios at hour 7 indicate that the reliability reduces while the available linepack increases. Even for a value of *a* of 0.5, the reliability at hour 7 still decreases. This indicates that although reducing the contract pressure can increase the available natural gas stored in pipelines, however, the failure probability can still increase at some hours due to the difference between the available linepack and the increased natural gas demand of those hours.

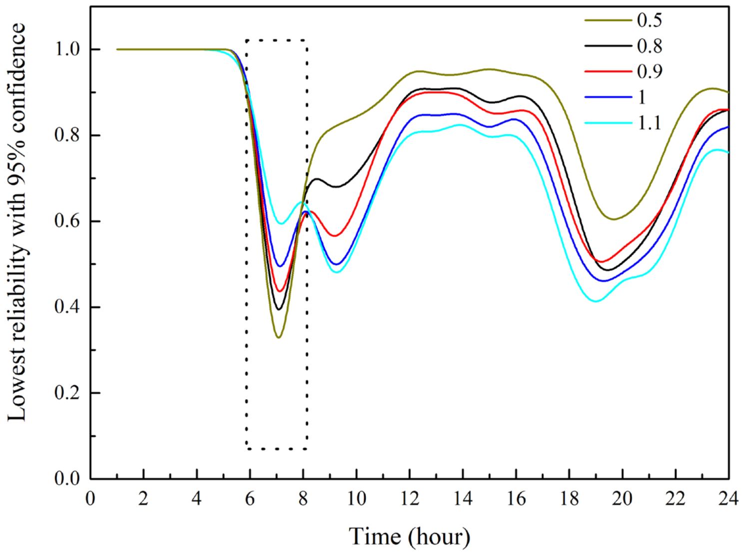


Fig. 12. Lowest reliability with 95% confidence in different scenarios

(0.5,0.8,0.9,1,1.1 represent the value of *a*)

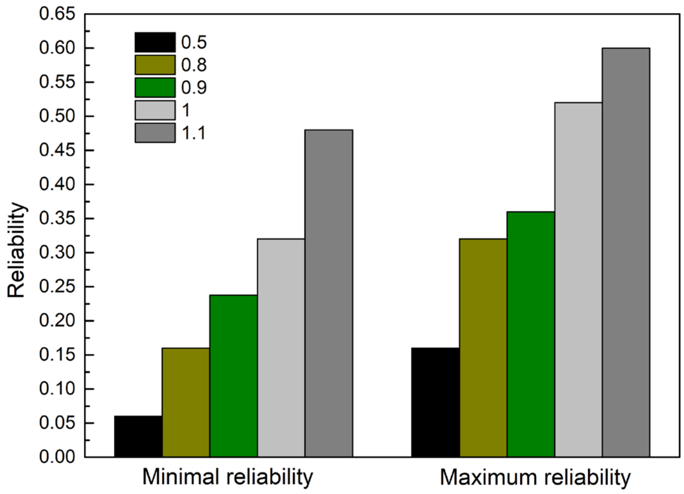


Fig. 13. The range of reliability with 95% confidence at hour 7 in different scenarios

(0.5,0.8,0.9,1,1.1 represent the value of *a*)

Increasing the maximum allowable pressure in natural gas pipeline networks can also increase the available linepack (we considered $b \cdot P_{1\max}$ as the maximum allowable pressure, with *b* taking values in the range (0.7-1.3) instead of the original maximum allowable pressure). As shown in Fig. 14, the general tendency is that reliability can be improved by increasing the maximum permissible pressure. However, at hour 7, the reliability decreases even with the increase of maximum permissible pressure, up to *b* values of 1.3. The results are similar to the results in Fig. 12. When the maximum allowable pressure exceeds a specific value, the available linepack can be sufficient to satisfy the increase of natural gas demand.

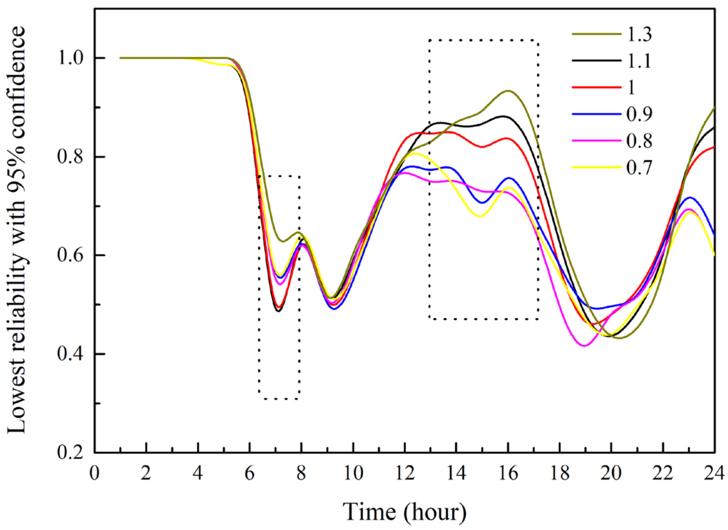


Fig. 14. Lowest reliability with 95% confidence in different scenarios

(0.7,0.8,0.9,1,1.1,1.3 represent the value of *b*)

In Fig. 15, we increase the maximum allowable pressure and reduce the contract pressure at the same time. It is shown that changing these two parameters can improve the reliability at hour 7, when *a*=0.8 and *b*=1.2. There is, then, a critical point in which the available pressure linepack is sufficient to meet the demand at hour 7.

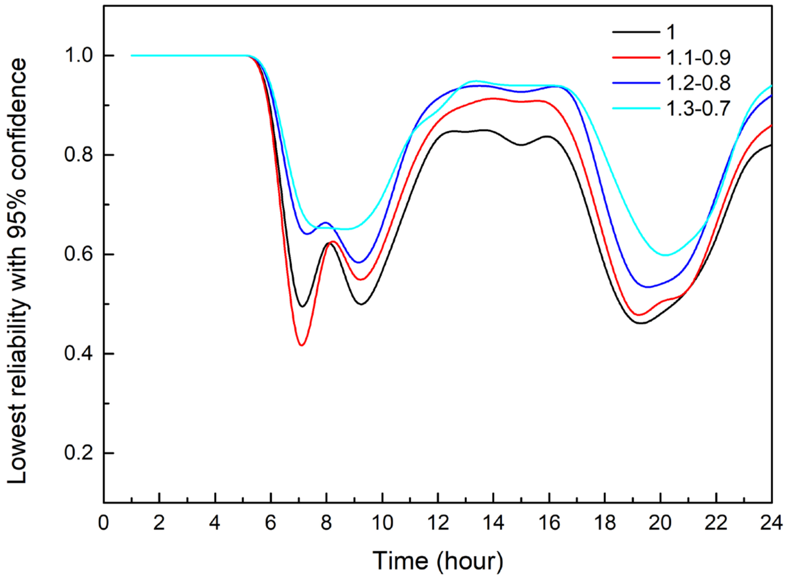


Fig. 15. Lowest reliability with 95% confidence in different scenarios

(Left numbers represent the value of *b* and right numbers represent the value of *a*)

The linepack can improve the reliability of the IES, as discussed above. However, reliability can be reduced even with the increase of available linepack at some time instances and some risky points can occur. Depending on the strategies used in practice, the flow rate at the inlet of a pipeline can be constant, because the available linepack in the pipeline can meet the demand changes; then, the linepack may decrease at some time steps and be unavailable to satisfy demand changes at the next time step, which can cause a reduction of reliability.

## 5 Conclusions

This paper proposes a novel framework for the assessment of supply reliability of IESs. In this framework, a quasi-steady-state model is used to realistically describe the dynamic process of IES with high calculation efficiency and accounting for the available linepack. A model that combines the statistical structure of the empirical copula with the machine learning method of SAE is proposed to generate time-series data for dynamic reliability assessment. The model allows describing the inter-correlations between uncertain factors and time-dependent relationships for each variable. Three case studies are considered for the application of the proposed framework and the main findings are as follows:

(1) Compared to the simulation results from the dynamic model and steady-state model, the quasi-steady-state model is capable of improving the accuracy of the supply reliability assessment of IES, as the requirement of the contract pressure of the system and the operational stability are guaranteed.

(2) The relationships internal to the time series data are strong during the day whereas inter-correlations between uncertain factors are strong during the peak hours. When inter-correlations between uncertain factors and the relationships in the time series data of the relevant process variables are strong, the impact on the accuracy of reliability estimation is significant.

(3) The linepack in natural gas pipeline networks can contribute to improving the reliability of supply in IES, as the available linepack in the pipeline can help meeting the demand changes. However, some critical instances can occur in the management strategy of linepack operation, because the linepack might become unavailable to satisfy demand changes at the next time step.

In future work, it is worthy of further study to consider the inter-correlation between renewable resources, different kinds of energy demand, and human behaviour in operation. Besides, the impact of demand-response management and storage devices on the reliability assessment will be analysed in more detail.

## Acknowledgement

This work is supported by National Natural Science Foundation of China [grant number 51904316], and the research fund provided by China University of Petroleum, Beijing [grant number 2462018YJRC038, 2462020YXZZ045]. We appreciate the contributions of the editors and reviewers to the improvement of this work.

## Appendix A

### A.1 AC electric power model

An AC power flow model is used to simulate the electric power network operation [57], in which the active power $P_{ij}$ and reactive power $Q_{ij}$ at branch $ij$ are calculated as follows (Eq.A1):

$$\begin{aligned} P_{ij} &= (g_{si} + g_{ij}) - g_{ij} V_i V_j \cos\theta_{ij} - b_{ij} V_i V_j \sin\theta_{ij} \\ Q_{ij} &= -(b_{si} + b_{ij}) + b_{ij} V_i V_j \cos\theta_{ij} - g_{ij} V_i V_j \sin\theta_{ij} \end{aligned} \tag{A1}$$

where $g_{ij}$ and $b_{ij}$ are the conductance and susceptance of nodal admittance matrix, respectively; $g_{si}$ and $b_{si}$ are the conductance and susceptance to the ground of node $i$, respectively; $\theta_{ij}=\theta_i-\theta_j$, $\theta$ is the angle of voltage; $V$ is bus voltage.

### A.2 Basic natural gas pipeline networks model

A steady-state natural gas pipeline networks model is combined with the LBPAM to describe the gas flow dynamics with reduced computational burden.

Assuming that the flow is isothermal and the pipeline has no elevation changes, the gas flow $Q_{gas,mn}$ of pipeline $mn$ can be written as (Eq. A2) [12]:

$$P_m^2 - P_n^2 = C_{mn} Q_{gas,mn}^2 \tag{A2}$$

where $P_m$ and $P_n$ denote the pressure at nodes $m$ and $n$; $C_{mn}$ indicates the hydraulic resistance coefficient of pipeline $mn$, which can be calculated as (Eq. A3):

$$C_{mn} = \left\{ C \left( \frac{T_\mathrm{b}}{P_\mathrm{b}} \right) D_{mn}^{2.5} \left( \frac{1}{L_{mn} \gamma_\mathrm{G} T_{\mathrm{a},mn} Z_\mathrm{a} f_{mn}} \right)^{0.5} E_{\mathrm{p},mn} \right\}^{-1} \tag{A3}$$

where $D_{mn}$ represents the diameter of the pipeline $mn$; $T_\mathrm{b}$ and $P_\mathrm{b}$ denote the gas temperature and pressure at base conditions, respectively; $L_{mn}$ denotes the length of pipeline $mn$; $\gamma_\mathrm{G}$ is the specific gravity; $Z_\mathrm{a}$ represents the average compressibility factor; $E_{\mathrm{p},mn}$ is the pipeline efficiency; the friction factor $f_{mn}$ can be obtained as (Eq. A4):

$$\frac{1}{f_{mn}} = -2 \log_{10} \left( \frac{\varepsilon_{mn}}{3.71 D_{mn}} \right) \tag{A4}$$

where $\varepsilon_{mn}$ donates the absolute roughness of pipeline $mn$.

The compressor is used to provide energy for achieving the gas transmission requirements, and its power consumption can be calculated as (Eq. A5):

$$HP = \frac{Q_{GC} Z_a R T_s}{\eta_s} \; {}_s \frac{k_v}{k_v - 1} \left[ \left( \frac{p_n}{p_m} \right)^{\frac{k_v - 1}{k_v}} - 1 \right] \tag{A5}$$

where $T_s$ is the suction temperature of the compressor; $k_v$ is the specific heat ratio of natural gas; $\eta_s$ is the efficiency of the compressor.

Linepack refers to the volume of gas that can be stored in a gas pipeline. Due to the compressibility of gas, more gas can be compressed into a fixed volume. This means that the volume of gas injected into a pipeline can be higher than the volume of gas withdrawn from the upstream. The inventory capacities can be defined as (Eq. A6):

$$Vs = Vs_{\max} - Vs_{\min} = \frac{\pi D^2}{4} \frac{P_{pj}^{\max} - P_{pj}^{\min}}{P_0} \frac{T_0}{T_a Z_a} L_{mn} \tag{A6}$$

where $P_0$ and $T_0$ are the pressure and temperature of natural gas at standard conditions, respectively; $P_{pj}^{\max}$ and $P_{pj}^{\min}$ are the maximum average pipeline pressure and minimum average pipeline pressure, which can be obtained as (Eq. A7):

$$\begin{aligned} P_{pj}^{\max} &= \frac{2}{3} \left( P_{1\max} + \frac{P_{2\max}^2}{P_{1\max} + P_{2\max}} \right) \\ P_{pj}^{\min} &= \frac{2}{3} \left( P_{1\min} + \frac{P_{2\min}^2}{P_{1\min} + P_{2\min}} \right) \end{aligned} \tag{A7}$$

where $P_{1\min}$ and $P_{1\max}$ are the minimum and maximum pressure values at the inlet of the pipeline, respectively; $P_{2\min}$ and $P_{2\max}$ are the minimum and maximum pressure values at the outlet of the pipeline, respectively.

### A.3 Energy conversion modelling

Gas-fired power generation (GPG) and Power to Gas (P2G) systems are installed for energy conversion between the natural gas pipeline networks and the power system.

The gas consumption for generating power by GPG can be calculated as (Eq. A8):

$$Q_{d,GPG} = \frac{3600 \cdot P_{g,GPG}}{\eta_{GPG} LHV} \tag{A8}$$

where $\eta_{\mathrm{GPG}}$ is the energy efficiency of the power plant; *LHV* denotes the lower heating value of gas, ranging from 35.40 to 39.12 MJ/m$^3$.

The power to gas (P2G) system can convert power to natural gas, which can then be injected into the natural gas pipeline networks. The relationship between the power consumption $P_{\mathrm{P2G}}$ and the gas generation $Q_{\mathrm{P2G}}$ can be defined as follows (Eq. A9):

$$Q_{\mathrm{P2G}} = \left( \frac{3600\eta_{\mathrm{P2G}}}{LHV} \right) \cdot P_{\mathrm{P2G}} \tag{A9}$$

where $\eta_{\mathrm{P2G}}$ is the energy efficiency of P2G.

**2.1.4 Renewables generation**

The power generated by renewable resources such as wind and solar, can affect the operational reliability of IES. The output of the wind farm depends on the wind speed and can be calculated as (Eq. A10):

$$P_{g,wind} = \begin{cases} P_r & V_r \le V_w < V_{co} \\ P_r \times \dfrac{V_w - V_{ci}}{V_r - V_{ci}} & V_{ci} \le V_w < V_r \\ 0 & V_w < V_{ci} \text{ or } V_w > V_{co} \end{cases} \tag{A10}$$

where $P_{g,wind}$ is the active power of the wind farm at wind speed $V_w$; $P_r$ denotes the rated power of the wind turbine; $V_r$, $V_{ci}$ and $V_{co}$ represent the rated, the cut-in and cut-out wind speeds, respectively.

The production of a PV can be defined as (Eq. A11):

$$P_{pv} = P_{pv,r}\eta_{pv} \frac{G}{G_r}\left[1 + \gamma\left(T_c - T_{c,r}\right)\right] \tag{A11}$$

where $P_{pv}$ is the generated power; $P_{pv,r}$ denotes the rated capacity of PV; $\gamma$ is the temperature coefficient; $T_{c,r}$ and $T_c$ are the tested and current temperatures, respectively; $\eta_{pv}$ is the efficiency of PV; $G$ and $G_{\mathrm{r}}$ are the real and tested solar radiation values, respectively.

**Appendix B**

**B1 Empirical copula**

Let $H$ be a continuous multivariate cumulative distribution function with uniform marginal distribution functions. Base on the definition of copula, the joint distribution function $H$ can be formed as follows (Eq. B1) [58]:

$$H\left(x_1,\ ...,\ x_p\right)=C\left(F_1(x_1),\ ...,\ F_p(x_p)\right) \quad x_i \in \mathbb{R}^p \tag{B1}$$

where $C$ is called the copula associated with $H$. $C$ is a multivariate distribution function on [0, 1] $^p$, whose marginals are standard uniform distributions on [0, 1]. Then, the copula $C$ is unique, and the functions can be related by (Eq. B2):

$$C\left(\boldsymbol{u}\right)=H\left(F_1^-\left(u_1\right),\ ...,\ F_p^-\left(u_p\right)\right) \quad \boldsymbol{u}\in[0,1]^p \tag{B2}$$

where $F_p^-$ donates the generalised quantile functions of $F_p$. The generalised inverse can be defined as:

$$F_p^-\left(u_p\right)=\inf\left\{x\in\mathbb{R}\middle|F\left(x\right)\geq u_p\right\} \tag{B3}$$

The density function $h$ associated with $H$ can be obtained (Eq. B4):

$$h\left(x_1,\ ...,\ x_p\right)=c\left(F_1\left(x_1\right),\ ...,\ F_p\left(x_p\right)\right)\times\prod_{i=1}^{p}f_i\left(x_i\right) \tag{B4}$$

The empirical copula is a fundamental tool for statistical inference on copulas [59]. Based on $H$, we construct the empirical distribution function, which can be defined as (Eq. B5):

$$\mathbb{H}_n\left(\boldsymbol{x}\right)=\frac{1}{n}\sum_{i=1}^{p}\mathbb{I}\left\{\boldsymbol{X}_i\leq\boldsymbol{x}\right\} \quad \boldsymbol{x}\in\mathbb{R} \tag{B5}$$

The related empirical copula is defined as (Eq. B6):

$$\mathbb{C}_n\left(\boldsymbol{u}\right)=\mathbb{H}\left(\mathbb{F}_{n1}^-\left(u_{n1}\right),\ ...,\ \mathbb{F}_{np}^-\left(u_{np}\right)\right) \quad \boldsymbol{u}\in[0,1]^p \tag{B6}$$

Then the empirical copula process can be obtained (Eq. B7):

$$\mathbb{Z}_n(\boldsymbol{u})=\sqrt{p}\left(C_n\left(\boldsymbol{u}\right)-C\left(\boldsymbol{u}\right)\right) \tag{B7}$$

**B2 The stacked auto-encoder model**

The main idea of the model is to reconstruct the input at the end of the Autoencoder and this process can be conducted by encoding and decoding parts. Auto-encoder is a simple network for deep neural network pre-training and SAE is obtained by the successive stacking of autoencoders.

The encoder maps the inputs $x \in R^n$ to the hidden layers and captures the features of the data. The decoder performs a self-reconstruction process from the hidden layer as shown in Eqs. (B8-B9) [55]:

$$\mathbf{z} = E(\mathbf{x}, \boldsymbol{\theta}) \tag{B8}$$

$$\mathbf{x}' = D(\mathbf{z}, \boldsymbol{\theta}') \tag{B9}$$

where $\mathbf{x} \in \mathbf{R}^n$ and $\mathbf{x}' \in \mathbf{R}^n$ are the input data and reconstructed output, respectively; $\mathbf{z}$ is the latent representation. *E* and *D* represent the activation functions depending on the parameter $\boldsymbol{\theta}$ and $\boldsymbol{\theta}'$, respectively, including weight matrix and bias vector. The loss function, which can recreate the compressed features, is mathematically expressed as (Eq. B10):

$$L(\mathbf{x}, \mathbf{x}') = \left\| \mathbf{x} - \mathbf{x}' \right\|^2 \tag{B10}$$

Unlike the autoencoder, the numbers of input and output layers in SAE models are the same, and the number of input layers is greater than the number of hidden layers. Therefore, this model can generate new information by eliminating the noise and bring effective attributes with complex relationships.

References

[1] Wu J, Yan J, Jia H, Hatziargyriou N, Djilali N, Sun H. Integrated Energy Systems. Applied Energy. 2016;167(apr.1):155-7.
[2] Guelpa E, Bischi A, Verda V, Chertkov M, Lund H. Towards future infrastructures for sustainable multi-energy systems: A review. Energy. 2019.
[3] Yan R, Wang J, Lu S, Ma Z, Zhou Y, Zhang L, et al. Multi-objective two-stage adaptive robust planning method for an integrated energy system considering load uncertainty. Energy and Buildings. 2021;235:110741.
[4] Lund H, Østergaard PA, Connolly D, Mathiesen BV. Smart energy and smart energy systems. Energy. 2017;137:556-65.
[5] Lund H. Renewable heating strategies and their consequences for storage and grid infrastructures comparing a smart grid to a smart energy systems approach. Energy. 2018;151:94-102.
[6] Lund H, Thellufsen JZ, Sorknæs P, Mathiesen BV, Chang M, Madsen PT, et al. Smart energy Denmark. A consistent and detailed strategy for a fully decarbonized society. Renewable and Sustainable Energy Reviews. 2022;168:112777.
[7] Li R, Mahalec V. Greenhouse gas emissions reduction by cross-sector integration of energy systems: Optimal sizing of integrated entities. Energy Conversion and Management. 2021;248.
[8] Lynch M, Devine MT, Bertsch V. The role of power-to-gas in the future energy system: Market and portfolio effects. Energy. 2019;185:1197-209.
[9] Østergaard PA, Lund H, Thellufsen JZ, Sorknæs P, Mathiesen BV. Review and validation of EnergyPLAN. Renewable and Sustainable Energy Reviews. 2022;168:112724.
[10] Thellufsen JZ, Lund H, Sorknæs P, Østergaard PA, Chang M, Drysdale D, et al. Smart energy cities in a 100% renewable energy context. Renewable and Sustainable Energy Reviews. 2020;129.
[11] Connolly D, Lund H, Mathiesen BV. Smart Energy Europe: The technical and economic impact of one potential 100% renewable energy scenario for the European Union. Renewable and Sustainable Energy Reviews. 2016;60:1634-53.
[12] Zeng Q, Fang J, Li J, Chen Z. Steady-state analysis of the integrated natural gas and electric power system with bi-directional energy conversion. Applied Energy. 2016;184:1483-92.
[13] Lei Y, Hou K, Wang Y, Jia H, Zhang P, Mu Y, et al. A new reliability assessment approach for integrated energy systems: Using hierarchical decoupling optimization framework and impact-increment based state enumeration method. Applied Energy. 2018;210:1237-50.
[14] Fu X, Guo Q, Sun H, Zhang X, Wang L. Estimation of the failure probability of an integrated energy system based on the first order reliability method. Energy. 2017;134:1068-78.
[15] Shariatkhah M-H, Haghifam M-R, Parsa-Moghaddam M, Siano P. Modeling the reliability of multi-carrier energy systems considering dynamic behavior of thermal loads. Energy and Buildings. 2015;103:375-83.
[16] Li D, Zhang Q, Zio E, Havlin S, Kang R. Network reliability analysis based on percolation theory. Reliability Engineering & System Safety. 2015;142:556-62.
[17] Amrin A, Zarikas V, Spitas C. Reliability analysis and functional design using Bayesian networks generated automatically by an “Idea Algebra” framework. Reliability Engineering & System Safety. 2018;180:211-25.
[18] Su H, Zhang J, Zio E, Yang N, Li X, Zhang Z. An integrated systemic method for supply reliability assessment of natural gas pipeline networks. Applied Energy. 2018;209:489-501.
[19] Faza A. A probabilistic model for estimating the effects of photovoltaic sources on the power systems

reliability. Reliability Engineering & System Safety. 2018;171:67-77.
[20] Lund H, Arler F, Østergaard P, Hvelplund F, Connolly D, Mathiesen B, et al. Simulation versus Optimisation: Theoretical Positions in Energy System Modelling. Energies. 2017;10(7).
[21] Liu X, Wu J, Jenkins N, Bagdanavicius A. Combined analysis of electricity and heat networks. Applied Energy. 2016;162:1238-50.
[22] Wang Y, Cheng J, Zhang N, Kang C. Automatic and linearized modeling of energy hub and its flexibility analysis. Applied Energy. 2018;211:705-14.
[23] Qadrdan M, Wu J, Jenkins N, Ekanayake J. Operating strategies for a GB integrated gas and electricity network considering the uncertainty in wind power forecasts. IEEE Transactions on Sustainable Energy. 2013;5(1):128-38.
[24] Lan P, Han D, Xu X, Yan Z, Ren X, Xia S. Data-driven state estimation of integrated electric-gas energy system. Energy. 2022;252.
[25] Devlin J, Li K, Higgins P, Foley A. A multi vector energy analysis for interconnected power and gas systems. Applied Energy. 2017;192:315-28.
[26] Ding T, Xu Y, Wei W, Wu L. Energy Flow Optimization for Integrated Power-Gas Generation and Transmission Systems. IEEE Transactions on Industrial Informatics. 2019:1-.
[27] Chaudry M, Jenkins N, Strbac G. Multi-time period combined gas and electricity network optimisation. Electric Power Systems Research. 2008;78(7):1265-79.
[28] Fang J, Zeng Q, Ai X, Chen Z, Wen J. Dynamic Optimal Energy Flow in the Integrated Natural Gas and Electrical Power Systems. IEEE Transactions on Sustainable Energy. 2018;9(1):188-98.
[29] Xu X, Jia H, Chiang HD, Yu DC, Wang D. Dynamic modeling and interaction of hybrid natural gas and electricity supply system in microgrid. IEEE Transactions on Power Systems. 2015;30(3):1212-21.
[30] Qin X, Sun H, Shen X, Guo Y, Guo Q, Xia T. A generalized quasi-dynamic model for electric-heat coupling integrated energy system with distributed energy resources. Applied Energy. 2019;251.
[31] Duquette J, Rowe A, Wild P. Thermal performance of a steady state physical pipe model for simulating district heating grids with variable flow. Applied Energy. 2016;178:383-93.
[32] Pan Z, Guo Q, Sun H. Interactions of district electricity and heating systems considering time-scale characteristics based on quasi-steady multi-energy flow. Applied Energy. 2016;167:230-43.
[33] Wang LX, Zheng JH, Li MS, Lin X, Jing ZX, Wu PZ, et al. Multi-time scale dynamic analysis of integrated energy systems: An individual-based model. Applied Energy. 2019;237:848-61.
[34] Su H, Zio E, Zhang J, Li Z, Wang H, Zhang F, et al. A systematic method for the analysis of energy supply reliability in complex Integrated Energy Systems considering uncertainties of renewable energies, demands and operations. Journal of Cleaner Production. 2020;267:122117.
[35] Zio E, Delfanti M, Giorgi L, Olivieri V, Sansavini G. Monte Carlo simulation-based probabilistic assessment of DG penetration in medium voltage distribution networks. International Journal of Electrical Power & Energy Systems. 2015;64:852-60.
[36] A CW, A HX, A ZB, A GL, A CYJRE, Safety S. Fast supply reliability evaluation of integrated power-gas system based on stochastic capacity network model and importance sampling. 2021;208.
[37] Kannan V, Xue H, Raman KA, Chen J, Fisher A, Birgersson E. Quantifying operating uncertainties of a PEMFC – Monte Carlo-machine learning based approach. Renewable Energy. 2020;158:343-59.
[38] Kou Y, Bie Z, Li G, Liu F, Jiang J. Reliability evaluation of multi-agent integrated energy systems with fully distributed communication. Energy. 2021;224.
[39] Sansavini G, Piccinelli R, Golea LR, Zio E. A stochastic framework for uncertainty analysis in electric power transmission systems with wind generation. Renewable Energy. 2014;64:71-81.

[40] Fu X, Li G, Wang H. Use of a second-order reliability method to estimate the failure probability of an integrated energy system. Energy. 2018;161:425-34.
[41] Chi L, Su H, Zio E, Zhang J, Li X, Zhang L, et al. Integrated Deterministic and Probabilistic Safety Analysis of Integrated Energy Systems with bi-directional conversion. Energy. 2020;212.
[42] Fu X, Li G, Zhang X, Qiao Z. Failure probability estimation of the gas supply using a data-driven model in an integrated energy system. Applied Energy. 2018:232.
[43] Liu Z, Cui Y, Wang J, Yue C, Agbodjan YS, Yang Y. Multi-objective optimization of multi-energy complementary integrated energy systems considering load prediction and renewable energy production uncertainties. Energy. 2022;254.
[44] Yu L, Li YP, Huang GH, Fan YR, Nie S. A copula-based flexible-stochastic programming method for planning regional energy system under multiple uncertainties: A case study of the urban agglomeration of Beijing and Tianjin. Applied Energy. 2018;210:60-74.
[45] Chi L, Su H, Zio E, Qadrdan M, Li X, Zhang L, et al. Data-driven reliability assessment method of Integrated Energy Systems based on probabilistic Deep Learning and Gaussian Mixture Model-Hidden Markov Model. Renewable Energy. 2021.
[46] Clegg S, Mancarella P. Integrated Modeling and Assessment of the Operational Impact of Power-to-Gas (P2G) on Electrical and Gas Transmission Networks. IEEE Transactions on Sustainable Energy. 2015;6(4):1234-44.
[47] Alabdulwahab A, Abusorrah A, Zhang X, Shahidehpour M. Coordination of interdependent natural gas and electricity infrastructures for firming the variability of wind energy in stochastic day-ahead scheduling. IEEE Transactions on Sustainable Energy. 2015;6(2):606-15.
[48] Wei Z, Chen S, Sun G, Wang D, Sun Y, Zang H. Probabilistic available transfer capability calculation considering static security constraints and uncertainties of electricity–gas integrated energy systems. Applied Energy. 2016;167:305-16.
[49] Ren Z, Li W, Billinton R, Yan W. Probabilistic Power Flow Analysis Based on the Stochastic Response Surface Method. IEEE Transactions on Power Systems. 2016;31(3):2307-15.
[50] Kunstmann H, Mauder M, Laux P, Soltani M. Spatiotemporal variability and empirical Copula-based dependence structure of modeled and observed coupled water and energy fluxes. Hydrology Research. 2018;49(5):1396-416.
[51] Bhatti MI, Do HQ. Recent development in copula and its applications to the energy, forestry and environmental sciences. International Journal of Hydrogen Energy. 2019;44(36):19453-73.
[52] Fu X, Sun H, Guo Q, Pan Z, Xiong W, Wang L. Uncertainty analysis of an integrated energy system based on information theory. Energy. 2017;122:649-62.
[53] Mu Y, Wang C, Cao Y, Jia H, Zhang Q, Yu X. A CVaR-based risk assessment method for park-level integrated energy system considering the uncertainties and correlation of energy prices. Energy. 2022;247.
[54] Shukur OB, Lee MH. Daily wind speed forecasting through hybrid KF-ANN model based on ARIMA. Renewable Energy. 2015;76:637-47.
[55] İrsoy O, Alpaydın E. Unsupervised feature extraction with autoencoder trees. Neurocomputing. 2017;258:63-73.
[56] Hammerschmitt BK, Guarda FGK, Lucchese FC, Abaide AdR. Complementary thermal energy generation associated with renewable energies using Artificial Intelligence. Energy. 2022;254.
[57] Martinez-Mares A, Fuerte-Esquivel CR. A unified gas and power flow analysis in natural gas and electricity coupled networks. IEEE Transactions on Power Systems. 2012;27(4):2156-66.
[58] A.Sklar. Fonctions de répartition à n dimensions et leurs marges. Publications de l'Institut Statistique

de l'Université de Paris. 1959;8:229–31.
[59] Bücher A, Volgushev S. Empirical and sequential empirical copula processes under serial dependence. Journal of Multivariate Analysis. 2013;119:61-70.